Electronic Supplementary Information

Materials characterization

X-ray diffraction (XRD) patterns were carried out to analyze the crystal phases of the samples on a Bruker D8 Advance X-ray instrument (Cu $K_{\alpha 1}$ radiation, λ=1.5406 Å) with a voltage of 40 kV and a current of 40 mA. The Fourier transform infrared (FTIR) spectrum was collected on Nicolet IS50 FTIR spectrometer (Thermo SCIENTIFIC). Field-emission scanning electron microscope (FESEM; Helios G4 CX) and transmission electron microscope (TEM; JEOL, JEM-2010) were used to analyze the morphology and structure of the samples. The composition of the samples was determined by energy-dispersive X-ray spectroscopy (EDX) attached to scanning electron microscope (SEM; Quanta 250). X-ray photoelectron spectroscopy (XPS) and ultraviolet photoelectron spectroscopy (UPS) were carried out on a PHI Quantum 2000 XPS system with C 1s binding energy (284.6 eV) as the reference and He I excitation energy (21.22 eV) as the monochromatic light source. N_2 adsorption–desorption isotherms characterizations were conducted on a Micromeritics ASAP2020 under liquid nitrogen temperature (77 K). UV-vis diffuse reflectance spectra (DRS) were obtained using a Varian Cary 500 UV-vis spectrometer using $BaSO_4$ as a reference. The photoluminescence (PL) characterizations were carried out on Hitachi F-7000 spectrophotometer at room temperature. The fluorescence lifetime was determined by recording the time-resolved fluorescence emission spectra in a Deltapro Fluorescence Lifetime System. In situ electron spin resonance (ESR) measurement was carried out on a Bruker A300 and a 300 W xenon (Xe) lamp ($\lambda \geqslant 420$ nm) was used as the light

source.

Photoelectrochemical measurement

The electrochemical measurement was carried out on Metrohm Autolab Electrochemical System, using a conventional three electrodes cell with Pt electrode and Ag/AgCl electrode as the counter electrode and reference electrode, respectively. Typically, 5 mg of the sample was dispersed in N, N-dimethylformamide (1 mL) by sonication to obtain a mixture. Then, the mixture was spread on the FTO glass with an area of ca. 0.25 cm^2 and dried at room temperature in the air. The transient photocurrent response spectra were conducted in Na_2SO_4 aqueous solution (0.2 M) with a 300 W xenon lamp ($\lambda \geq 420$ nm) as the light source. Electrochemical impedance spectroscopy (EIS) measurement was conducted at the open circuit potential and 1 mM $K_3[Fe(CN)_6]$, 1 mM $K_4[Fe(CN)_6]$ and 0.1 M KCl mixed solution was used as the electrolyte solution.

Photocatalytic H_2 evolution

The photocatalytic H_2 evolution reaction was carried out in closed quartz vessel equipped with Labsolar-6A all-glass automatic online trace gas analysis system (Perfectlight, Beijing). Typically, 40 mg photocatalyst was dispersed in 0.55 M Na_2S and 0.15 M Na_2SO_3 mixed solution (100 mL). Then, the system was stirred and under vacuum for 20 min. The temperature of the reaction was maintained at 10 ^{o}C using a circulating condensing unit. The light source was a 300 W Xe lamp with a 420 nm long-pass cutoff filter. Lastly, the amount of H_2 was determined by Agilent 7820A gas chromatography (GC) equipped with a thermal conductive detector (TCD) and a 5 Å

molecular sieve column, using the Ar as carrier gas. Other reaction conditions were the same as those of the typical reaction. Besides, other typical sacrificial agents (e.g., lactic acid, trolamine and methanol) were also used to evaluate the photocatalytic performance of the $NiTiO_3/Cd_{0.5}Zn_{0.5}S$ photocatalyst under otherwise identical conditions.

The apparent quantum yield (AQY) test was also performed under the conditions mentioned above, except that the filter was used a band-pass filter (*i.e.*, 400, 420, 450, and 500 nm). The AQY was calculated as follow:

$$\text{AQE} = \frac{2 \times \textit{the number of generated } H_2 \textit{ molecules}}{\textit{the number of incident photons}} \times 100\% = \frac{2 \times n \times N_A \times h \times c}{I \times S \times t \times \lambda} \times 100\% \quad \text{(Eq1)}^{1}$$

n is the amount of H_2 molecular, N_A is Avogadro constant, h is the Planck constant, c is the speed of light, I is the intensity of light source, S is the illumination area, t is the photoreaction time, and λ is the wavelength of the monochromatic light.

DFT calculation methods

The density function theory (DFT) calculation was performed using Vienna Ab-initio Simulation Package (VASP) code[2,3]. According to the experiment fact, two 8-layer atoms $Cd_{0.5}Zn_{0.5}S$ and $NiTiO_3$ models were established and the (100) and (104) crystal planes were exposed respectively, in which the top 4 layers of atoms were relaxed during the calculation and the other atoms were fixed to simulate the bulk phase. In addition, a 20 Å–thick vacuum layer was introduced to prevent the interaction between two adjacent slabs. The exchange-correlation function was utilized by generalized gradient approximation–Perdew–Burke–Ernzerhof (GGA-PBE) method[4]. The interaction between core and electron was described by the Projector Augmented Wave (PAW) method[5,6], and the cutoff energy was set to 450 eV. The Brillouin-zone integration was performed on 4×5×1 and 1×5×1 k-points of gamma center for $Cd_{0.5}Zn_{0.5}S$ and $NiTiO_3$ models, respectively. It can be considered that the accuracy of geometry optimization was reached when force of each atom was less than 0.02 eV/Å.

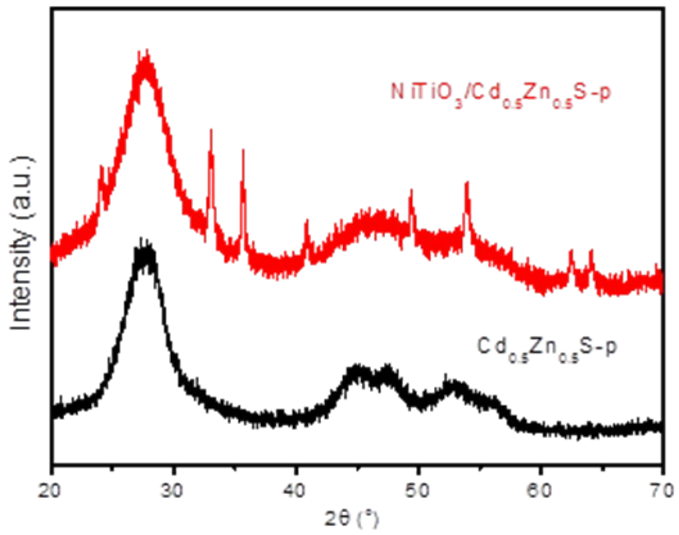

Fig. S1 XRD patterns of $Cd_{0.5}Zn_{0.5}S$-p and $NiTiO_3/Cd_{0.5}Zn_{0.5}S$-p.

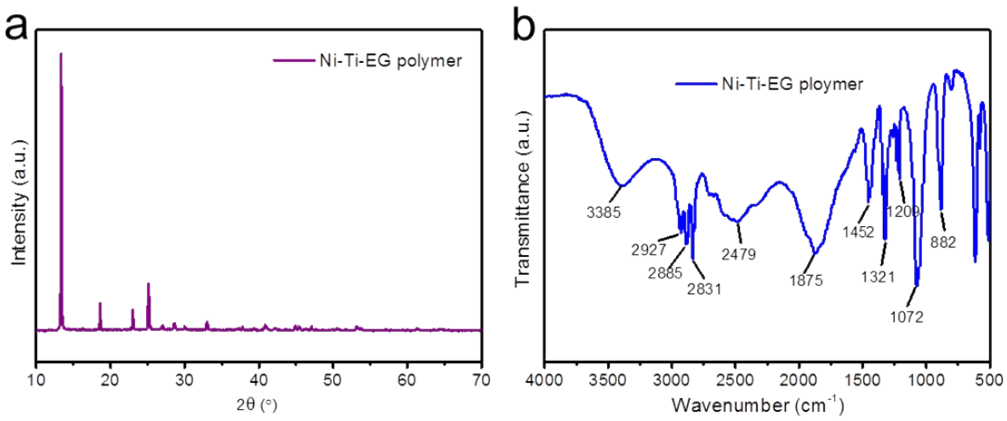

Fig. S2 (a) XRD pattern and (b) FTIR spectrum of Ni-Ti-EG polymer.

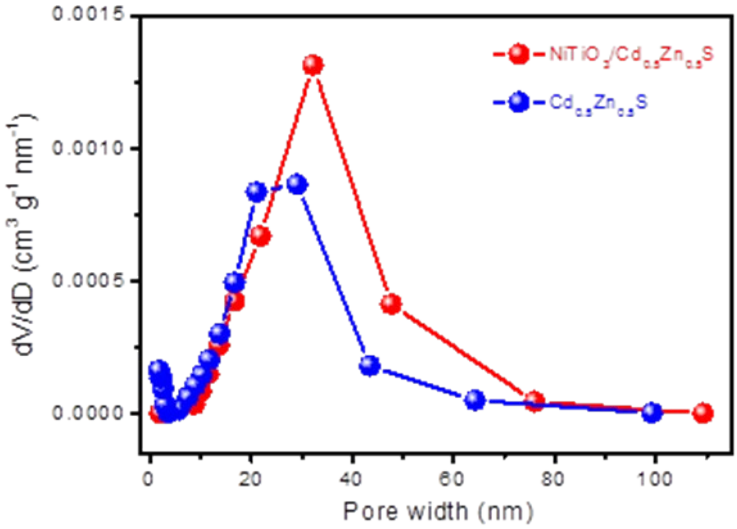

Fig. S3 The pore size distribution plots of $Cd_{0.5}Zn_{0.5}S$ and $NiTiO_3/Cd_{0.5}Zn_{0.5}S$.

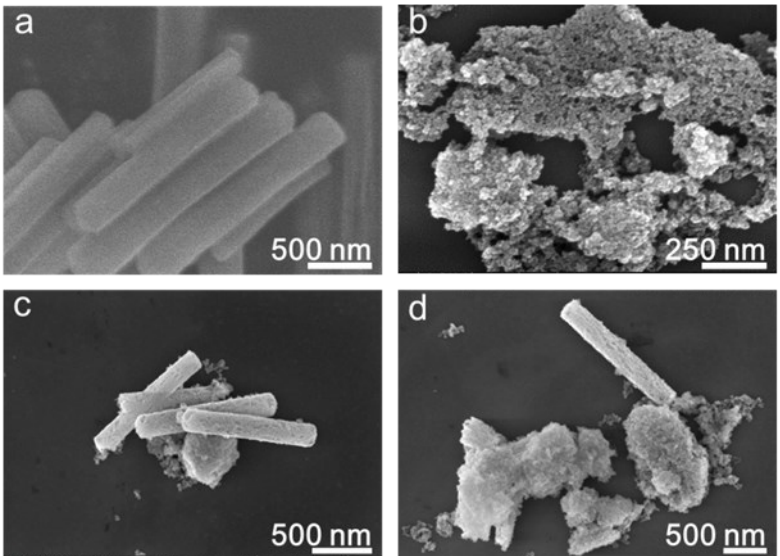

Fig. S4 FESEM images of (a) Ni-Ti-EG polymer, (b) $Cd_{0.5}Zn_{0.5}S$-p and (c and d) $NiTiO_3/Cd_{0.5}Zn_{0.5}S$-p.

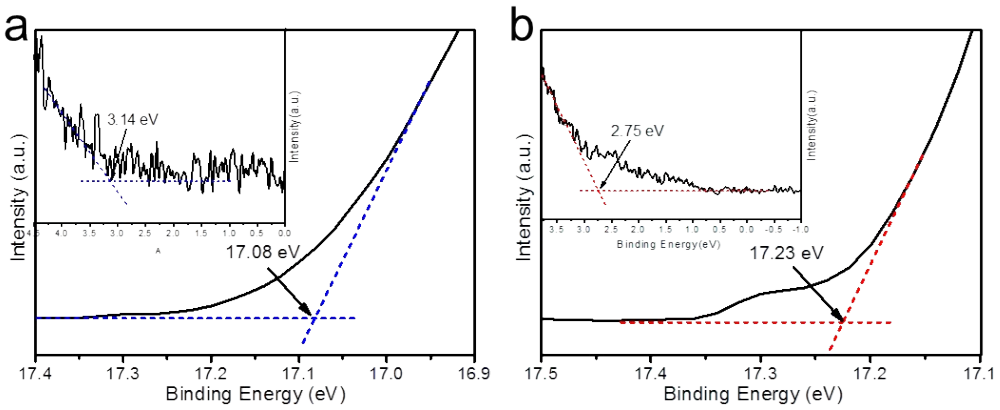

Fig. S5 UPS spectra of (a) $NiTiO_3$ and (b) $Cd_{0.5}Zn_{0.5}S$. The inset plots show the E_{edge} values.

We use UPS to determine the valence band maximum and the minimum of the conduction band.[7-9] E_{cutoff} and E_{edge} are obtained by applying linear intersection method. According to Eq2 and Eq3, the E_{VB} of $NiTiO_3$ and $Cd_{0.5}Zn_{0.5}S$ are calculated to be -7.28 and -6.75 V (*vs*. vacuum), respectively, by subtracting the width of the He I UPS spectrum from the excitation energy (21.22 eV). Simultaneously, the work functions (Φ) of $NiTiO_3$ and $Cd_{0.5}Zn_{0.5}S$ are calculated to be 4.14 and 3.99 eV (*vs*. vacuum), respectively. The relationship between the vacuum energy (E_{Vac}) and the reversible hydrogen electrode potential (E_{RHE}) follows the formula $E_{RHE} = -E_{Vac}-4.44$. The value of E_{RHE} is consistent with the normal hydrogen electrode potential (E_{NHE}) at pH = 0. Eventually, the E_{VB} of the $NiTiO_3$ and $Cd_{0.5}Zn_{0.5}S$ are calculated to be 2.43 and 1.89 V (*vs*. NHE, pH=7), respectively. On the basis of Eq4, the E_{CB} of $NiTiO_3$ and $Cd_{0.5}Zn_{0.5}S$ are located at 0.21 and -0.52 V (*vs*. NHE, pH=7), respectively.

$$h\nu = E_{cutoff} + \Phi \qquad \text{(Eq2)}$$

$$E_{VB} = E_{edge} + \Phi \qquad \text{(Eq3)}$$

$$E_{CB} = E_{VB} - E_g \qquad \text{(Eq4)}$$

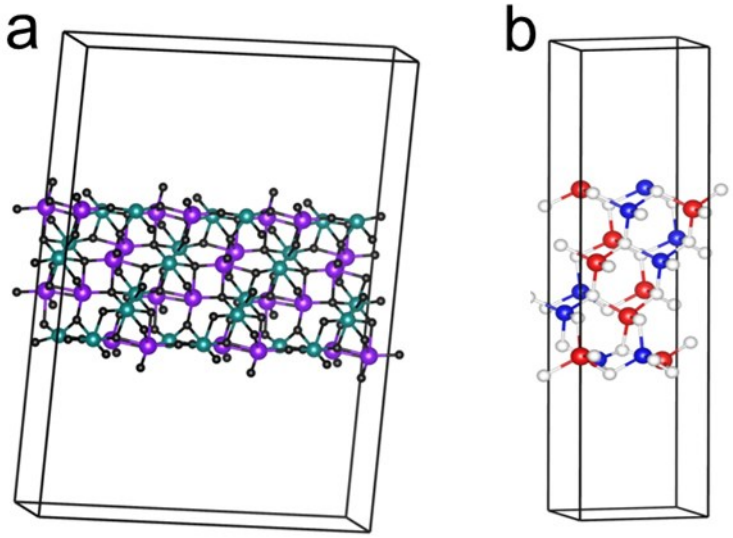

Fig. S6 Optimized crystal structures of the (a) $NiTiO_3$ (104) surface and (b) $Cd_{0.5}Zn_{0.5}S$ (100) surface. The purple, green, black, red, blue and white balls represent Ti, Ni, O, Cd, Zn and S atom, respectively.

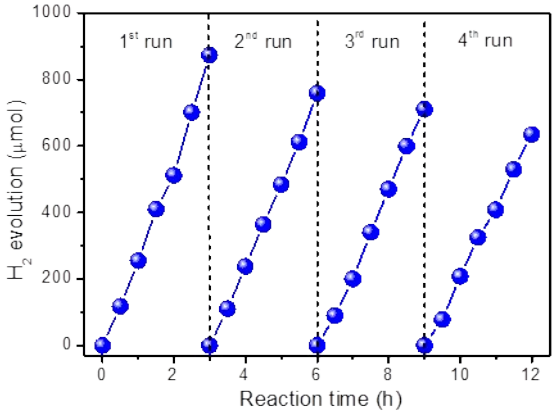

Fig. S7 Stability tests of pure $Cd_{0.5}Zn_{0.5}S$.

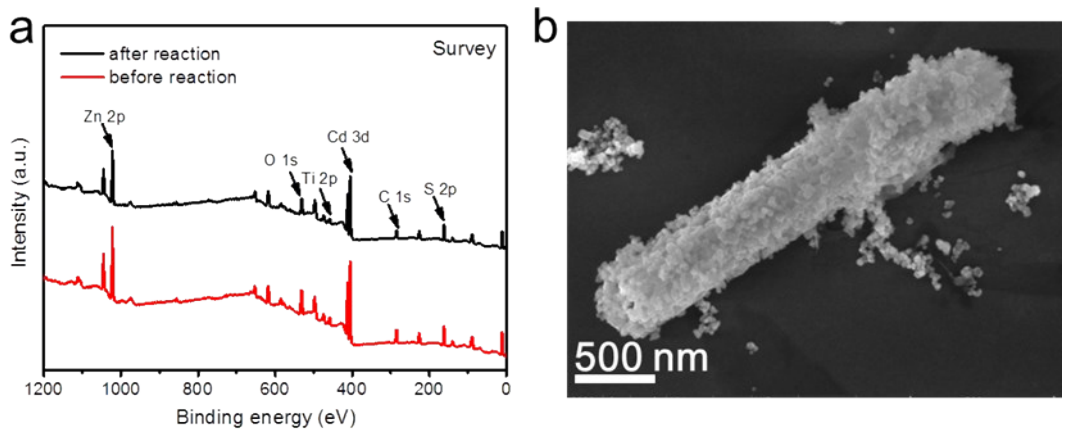

Fig. S8 (a) XPS spectra of $NiTiO_3/Cd_{0.5}Zn_{0.5}S$ before and after reaction. (b) SEM image of $NiTiO_3/Cd_{0.5}Zn_{0.5}S$ after reaction.

Table S1 Comparison of photocatalytic H_2 generation performance.

Catalyst	Sacrificial agent Cocatalyst	H_2 evolution rate (mmol h^{-1} g^{-1})	Reference
$NiTiO_3/Cd_{0.5}Zn_{0.5}S$	Na_2S-Na_2SO_3 /	26.47	This work
$Cd_{0.5}Zn_{0.5}S$@Halloysites	Na_2S-Na_2SO_3 Pt	25.67	10
$Cd_{0.5}Zn_{0.5}S$/OLC	Na_2S-Na_2SO_3 /	20.18	11
MoS_2–$Cd_{0.5}Zn_{0.5}S$	Lactic acid /	12.30	12
$Cd_{0.5}Zn_{0.5}S/BiVO_4$	Na_2S-Na_2SO_3 Pt	2.35	13
CdS/CoOx	Na_2S-Na_2SO_3 /	3.5	14
MoO_2-C/CdS	Lactic acid /	16.08	15
CdS-TiO_2	Na_2S-Na_2SO_3 Pt	1.50	16
Co/NGC@$ZnIn_2S_4$	TEOA /	11.27	17
MoS_2/Cu-$ZnIn_2S_4$	Ascorbic acid /	5.46	18

Supplementary References

1 Y. Li, B. Sun, H. Lin, Q. Ruan, Y. Geng, J. Liu, H. Wang, Y. Yang, L. Wang, K. Chiu Tam, *Appl. Catal.B Environ.,* 2020, **267**, 118702.

2 Kresse G.; Furthmüller, *J. Phys. Rev. B,* 1996, **54**, 11169-11186.

3 Kresse G.; Furthmuller, *J. Comp. Mater. Sci.,* 1996, **6**, 15-50.

4 Perdew, J. P.; Burke, K.; Ernzerhof, M. *Phys. Rev. Lett.,* 1996, **77**, 3865-3868.

5 Kresse G.; Joubert D. Phys. Rev. B, 1999, **59**, 1758-1775.

6 P.E. Blochl, *Phys Rev B,* 1994, **50**, 17953-17979.

7 M. Zhu, S. Kim, L. Mao, M. Fujitsuka, J. Zhang, X. Wang, T. Majima, *J. Am. Chem. Soc.,* 2017, **139**, 13234-13242.

8 F. Shi, Z. Geng, K. Huang, Q. Liang, Y. Zhang, Y. Sun, J. Cao, S. Feng, *Adv Sci (Weinh),* 2018, **5**, 1800575.

9 B. Su, L. Huang, Z. Xiong, Y. Yang, Y. Hou, Z. Ding, S. Wang, *J. Mater. Chem. A,* 2019, **7**, 26877-26883.

10 S. Lin, Y. Zhang, Y. You, C. Zeng, X. Xiao, T. Ma, H. Huang, *Adv. Funct. Mater.,* 2019, **29**, 1903825.

11 X. Zhou, X. Wang, X. Feng, K. Zhang, X. Peng, H. Wang, C. Liu, Y. Han, H. Wang, Q. Li, *ACS Appl Mater Interfaces,* 2017, **9**, 22560-22567.

12 S. Zhao, J. Huang, Q. Huo, X. Zhou, W. Tu, *J. Mater. Chem. A,* 2016, **4**, 193-199.

13 C. Zeng, Y. Hu, T. Zhang, F. Dong, Y. Zhang, H. Huang, *J. Mater. Chem. A,* 2018, **6**, 16932-16942.

14 Y. Liu, S. Ding, Y. Shi, X. Liu, Z. Wu, Q. Jiang, T. Zhou, N. Liu, J. Hu, *Appl. Catal.B Environ.,* 2018, **234**, 109-116.

15 W. Wei, Q. Tian, H. Sun, P. Liu, Y. Zheng, M. Fan, J. Zhuang, *Appl. Catal.B Environ.,* 2020, **260**, 118153.

16 Z. Jiang, K. Qian, C. Zhu, H. Sun, W. Wan, J. Xie, H. Li, P.K. Wong, S. Yuan, *Appl. Catal.B Environ.,* 2017, **210**, 194-204.

17 S. Wang, Y. Wang, S.L. Zhang, S.Q. Zang, X.W. Lou, *Adv. Mater.,* 2019, **31**, 1903404.

18 Y.-J. Yuan, D. Chen, J. Zhong, L.-X. Yang, J. Wang, M.-J. Liu, W.-G. Tu, Z.-T. Yu, Z.-G. Zou, *J. Mater. Chem. A,* 2017, **5**, 15771-15779.